ISSN 2350-1049

International Journal of Recent Research in Interdisciplinary Sciences (IJRRIS)
Vol. 10, Issue 2, pp: (41-57), Month: April - June 2023, Available at: www.paperpublications.org

GEOCHEMISTRY, CLASSIFICATION AND MATURITY OF THE EOCENE NANKA FORMATION SOUTH EAST, NIGERIA

Henry Y. Madukwe[1*], Matthew A. Adeniran[1], Paulinus N. Nnabo[2]

[1]Department of Geology, Ekiti State University Ado-Ekiti, Nigeria

[2]Department of Geology, Ebonyi State University, Abakaliki, Nigeria.

DOI: https://doi.org/10.5281/zenodo.7997489

Published Date: 02-June-2023

Abstract: **The geochemistry, classification and maturity of the Eocene Nanka Formation were investigated. The sandstones are non-calcareous, ferromagnesian potassic sandstones composed of sublitharenites and quartz arenites. Plot of SiO_2/Al_2O_3 against quartz / (feldspar + lithic fragments) indicates compositional maturity. SiO_2/Al_2O_3 and Fe_2O_3/K_2O values are high, implying mineralogical maturity and low degree of clayness and presence of stable mobile oxides. The minute alkali content indicates the near absence of feldspar and high chemical maturity. The ZTR values suggests that the sediments are mineralogically immature to sub mature, however, the mineralogical maturity index classifies the Nanka sandstone as mature to super mature. A decrease in the abundance of TiO_2, Fe_2O_3, CaO, Na_2O, MgO, MnO, K_2O, and Al_2O_3 as SiO_2 increases is due to chemical weathering and removal of these elements. There is no correlation between K_2O and TiO_2 suggesting a loss of K_2O and an indication of diagenetic alteration of feldspars. There is no correlation with Na; the extrapolated regression equation did not pass through the origin, suggesting minimal Na_2O contribution from the clay minerals. There is no correlation between TiO_2 and Al_2O_3 due to depositional process and granulometry; indicating that TiO_2 is not associated with phyllosilicates. TiO_2/Al_2O_3 ratio is low indicating that the sandstone matrix is composed of clay minerals. There is no correlation between K_2O and Al_2O_3 due to changes in the quartz-matrix proportions reflecting the grading. The Al—Ti—Zr ternary plot and the wide range of TiO_2/Zr variations, indicates compositional maturity, good sorting trend, rapid deposition and low to medium Zr concentration**

Keywords: **Eocene, mineralogical maturity index, quartz, sandstones, ZTR index.**

1. INTRODUCTION

Sedimentary rocks are derived from the weathering, erosion and transportation of already existing rock. materials and the chemical precipitation from solution including secretion by organisms in water. The eroded older materials are transported, deposited and lithified to form sedimentary rocks. Sedimentary rocks are classified into clastic and non-clastic. The clastic are also classified into terrigenous clastics and volcaniclastics. The terrigenous clastics sedimentary rocks are further categorized into mudrocks, sandstones and conglomerates (Nichols, 2009). Various classification schemes put forward by Blatt et al. (1972), Pettijohn et al. (1972), Folk (1974), Herron (1988) and Lindsey, (1999) was used as a basis for classification in this work. The Maturity of the sandstone under investigation was accomplished using parameters such as: The SiO_2/Al_2O_3 index, alkali content, ZTR index, mineralogical maturity index. The stability of mobile oxides can be determined by $Al_2O_3/(CaO+MgO+Na_2O+K_2O)$ ratio (Gill and Yamane, 1996). Detrital mineralogy can be determined by the Index of compositional variation (ICV) and ratio of K_2O/Al_2O_3 (Cox *et al.*, 1995). This investigation intends to carry out a classification and maturity status of the Eocene Nanka Formation based on inorganic geochemistry and mineralogy.

ISSN 2350-1049

International Journal of Recent Research in Interdisciplinary Sciences (IJRRIS)
Vol. 10, Issue 2, pp: (41-57), Month: April - June 2023, Available at: www.paperpublications.org

2. GEOLOGIC SETTING AND STRATIGRAPHY

The Anambra Basin in the south-eastern part of Nigeria (Fig. 1) is one of the intracratonic basins in Nigeria whose origin is related to the separation of Africa from South America and the opening of South Atlantic Ocean (Ofoegbu, 1982). The theory of the evolution of the basin have been discussed by some authors (e.g. Burke et al., 1972; Murat, 1972; Nwachukwu, 1972; Benkhelil, 1982; Benkhelil, 1987; Nwajide and Reijers, 1996; Obi, 2000). Subsequent evolution of the basin was influenced by some tectonic movements and the weight of accumulating sediments. Lithospheric thinning varying between 11.0 km and 27.0 km in a northeast southwesterly direction, while the thickness of the thermal lithosphere varies from 110 km to 128 km in a similar trend (Ekine and Onuoha, 2008). Sediment loading

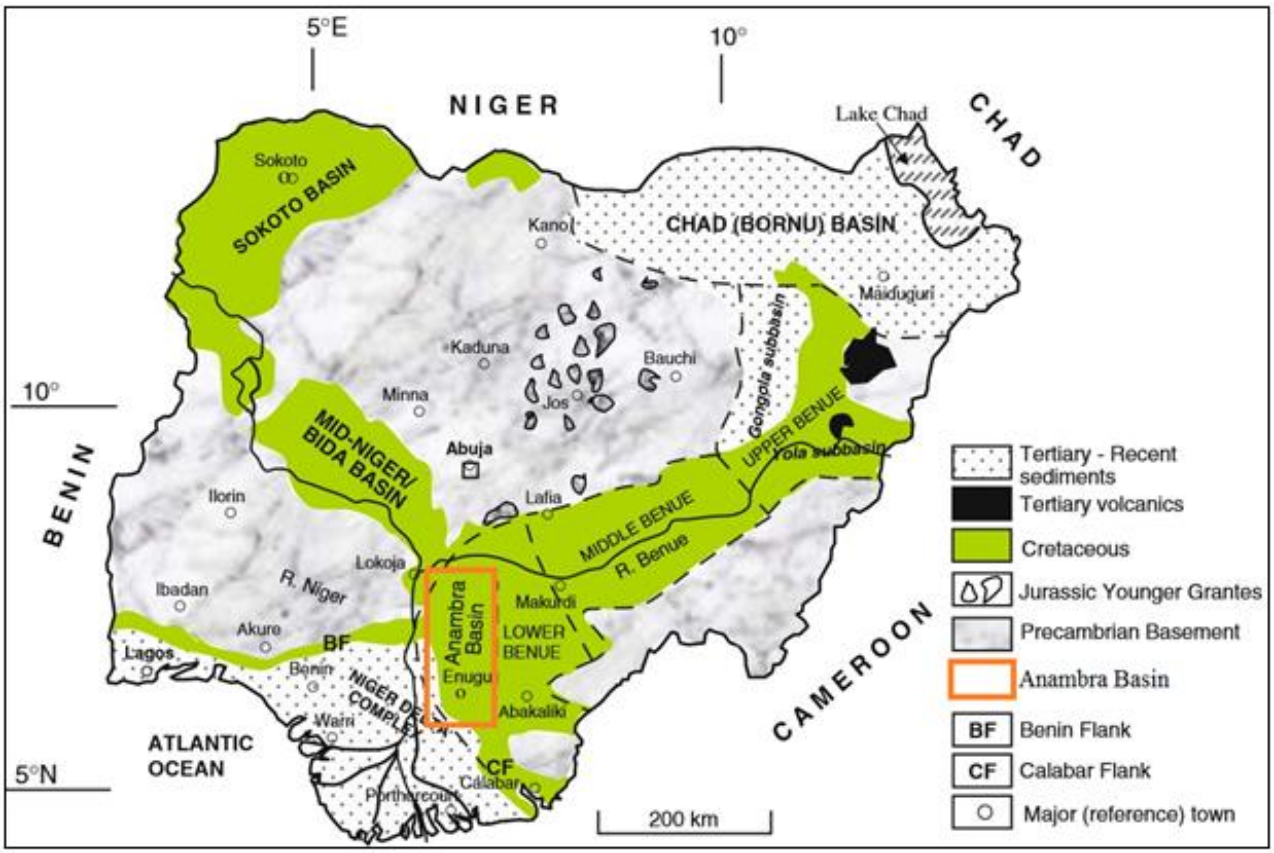

Figure 1. Schematic geological map of Nigeria showing the Basement Complex, Younger granites, and sedimentary basins (modified from Obaje, 2009).

which contributed about 43% of the total subsidence was identified as the dominant factor for subsidence particularly in the southwestern and deeper parts of the basin, whereas thermal subsidence accounts fora greater part of the total subsidence in the north northeastern parts and about an average of 33% of the total subsidence (Ekine and Onuoha, 2008). The basin is situated west of the lower Benue Trough and often considered newest formation from the Benue Trough (Obaje, 2009). The Basin is bordered to the north by Bida Basin and Northern Nigeria Massif, to the East by Benue Trough, to the west by West African Massif and to the south by the Niger Delta Complex; it is bounded to the south by the Niger Delta Basin hinge line (Shirley and Gordian, 2013). According to Agagu and Adighije (1983) the Anambra basin has sediment thickness of about 12,000 metres in its thickest part comprising mainly sandstones, shales, limestones and coal seams. Ola-Buraimo and Akaegbobi (2013b) invalidated earlier conception that Anambra Basin is exclusively of post-Santonian sediments. They showed that pre-Santonian sediments as old as Albian in age are present in the basin, which were dated based on palynology. The Asu-River Group is the oldest facies (in the basin) dated Albian to Lower Cenomanian. This is overlain by Eze-Aku Formation dated Upper Cenomanian to Turonian age; further overlain by the Awgu Formation dated as Coniacian. Table 1 is an outline of the stratigraphy of the Anambra basin; Figure 2 shows the location map of the study area. The stratigraphy of the Anambra basin has been examined by workers like Reyment (1965); Murat (1972); Dessauvagie (1975); Agagu et al. (1985); Ladipo (1986).

ISSN 2350-1049

International Journal of Recent Research in Interdisciplinary Sciences (IJRRIS)
Vol. 10, Issue 2, pp: (41-57), Month: April - June 2023, Available at: www.paperpublications.org

The Eocene stage was characterized by regressive phase that led to deposition of Ameki Group (Obi, 2000). The Ameki Group comprises the Ameki Formation; Nanka Formation and the Nsugbe Formation. The Eocene to Recent sediments are mainly represented in the southern parts of the basin where thicker colunms of the Paleocene Imo Shales are encountered (Ekine and Onuoha, 2008). Nwajide (1979 and 1980) established the Nanka Formation as the loose sand facies of the Ameki Group, that is flaser-bedded, fine to medium grained with few mudrock breaks. The Nanka Sands have been described by authors like: Simpson (1954), Reyment (1965), Adegoke (1969), Nwajide (1979). This study intends to determine the maturity and geochemistry of the Nanka sandstone, and classify the sediments based on existing classification schemes.

Table 1. Stratigraphy of the Anambra Basin (After Nwajide, 1990)

PERIOD	EPOCH	AGE	ABAKALIKI-ANAMBRA BASIN
PALAEOGENE	OLIGOCENE		Ogwashi-Asaba Formation
	EOCENE		Ameki/Nanka Formation/ Nsugbe Sandstone (Ameki Group)
	PALAEOCENE		Imo Formation Nsukka Formation
CRETACEOUS	Late	MAASTRICHTIAN	Ajali Formation Mamu Formation
		CAMPANIAN	Nkporo/Owelli Formation/Enugu Shale
		SANTONIAN	
		CONIACIAN	Agbani Sandstone/Awgu Shale
		TURONIAN	Eze Aku Group
		CENOMANIAN	
	EARLY	ALBIAN	Asu River Group

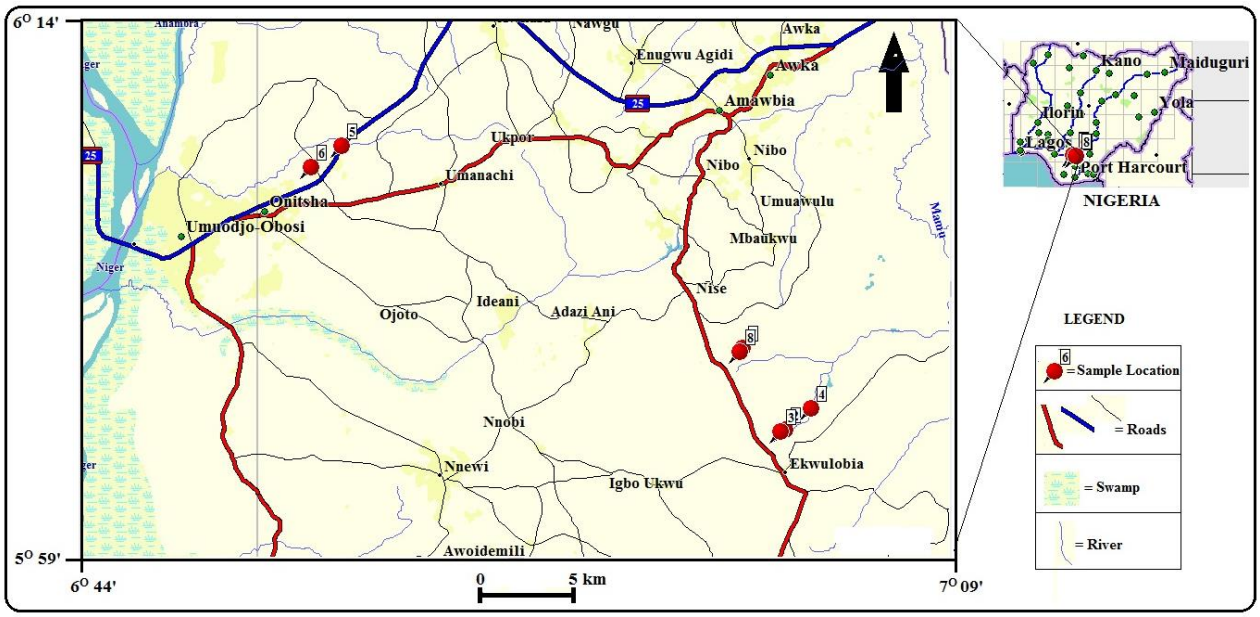

Figure 2. Location map of the study area.

3. METHODOLOGY

Ten samples were analyzed for major oxides, trace and rare earth elements using XRay Fluorescence (XRF) and LA-ICP-MS at Stellenbosch University, South Africa. Pulverised sandstone samples were analysed for major element using Axios instrument (PANalytical) with a 2.4 kWatt Rh X-ray Tube. The detailed procedures for sample preparation for the analytical technique are reported below.

Fusion bead method for Major element analysis:

- Weigh 1.0000 g ± 0.0009 g of milled sample
- Place in oven at 110 ºC for 1 hour to determine H2O+
- Place in oven at 1000 ºC for 1 hour to determine LOI
- Add 10.0000 g ± 0.0009 g Claisse flux and fuse in M4 Claisse fluxer for 23 minutes.
- 0.2 g of NaCO3 was added to the mix and the sample+flux+NaCO3 was pre-oxidized at 700 °C before fusion.
- Flux type: Ultrapure Fused Anhydrous Li-Tetraborate-Li-Metaborate flux (66.67 % $Li_2B_4O_7$ + 32.83 % $LiBO_2$) and a releasing agent Li-Iodide (0.5 % LiI).

The result returned eleven major elements, reported as oxide percent by weight (SiO_2, TiO_2, Al_2O_3, Fe2O3, MgO, MnO, CaO, Na_2O, K_2O, SO_3 and P_2O_5). Loss on Ignition (LOI) is a test used in XRF major element analysis which consists of strongly heating a sample of the material at a specified temperature, allowing volatile substances to escape or oxygen is added, until its mass ceases to change. The LOI is made of contributions from the volatile compounds of H_2O+, OH-, CO_2, F-, Cl-, S; in parts also K+ and Na+ (if heated for too long); or alternatively added compounds O2 (oxidation, e.g. FeO to Fe_2O_3), later CO_2 (CaO to $CaCO_3$). In pyro-processing and the mineral industries such as lime, calcined bauxite, refractories or cement manufacturing industry, the loss on ignition of the raw material is roughly equivalent to the loss in mass that it will undergo in a kiln, furnace or smelter. The trace and rare elemental data for this work was acquired using Laser Ablation inductively coupled plasma spectrometry

(LA-ICP-MS) analyses. The analytical procedures are as follows: Pulverised sandstone samples were analysed for trace element using LA-ICP-MS instrumental analysis. LA-ICP-MS is a powerful and sensitive analytical technique for multi elemental analysis. The laser was used to vaporize the surface of the solid sample, while the vapour, and any particles, were then transported by the carrier gas flow to the ICP-MS. The detailed procedures for sample preparation for both analytical techniques are reported below.

Pressed pellet method for Trace element analysis:

- Weigh 8 g ± 0.05 g of milled powder
- Mix thoroughly with 3 drops of Mowiol wax binder
- Press pellet with pill press to 15-ton pressure
- Dry in oven at 100 ºC for half an hour before analysing.

The petrography of the sandstone samples was determined by point-counting each thin section.

4. RESULTS AND DISCUSSION

4.1 Classification

Table 2 is the chemical composition of Nanka sandstone. Blatt et al., (1972), Pettijohn et al., (1972) and Herron (1988) examined the importance of the concentrations of these major oxides: silica and alumina, alkali oxides, and iron oxide plus magnesia as important variables for sandstone classification. The Nanka sandstone was classified based on the classification schemes of Pettijohn *et al.*, (1972); Blatt et al., (1972); Folk (1974); Herron (1988); and the geochemical classification of Lindsey, (1999). Figure 3 classified the Nanka sandstone as sublitharenite and subarkose with minor quartz arenites. Figure 4 classifies them mainly as Fe-sands with little portions on the quartz arenites and sublitharenites zones. According to Lindsey (1999), high MgO or Fe_2O_3 will yield anomalously high (Fe_2O_3+MgO)/(K_2O+Na_2O), causing the sample to plot outside the compositional fields for other sandstones. Figure 5 shows the Nanka sandstone plotting mainly in the sublitharenite field and few in the quartz arenites zone. The Nanka sandstone plotted only in ferromagnesian potassic sandstones zone (Fig. 6), this figure omitted sandstones with less than 5% Al_2O_3, therefore, quartz arenite is missing. Based on data from Pettijohn (1963; 1975), Lindsey (1999) revealed that average lithic arenites plotted in the ferromagnesian potassic sandstones zone, average greywacke plotted in the sodic sandstone zone while average arkose plotted in the potassic sandstones zone. Also, the Nanka sandstone is noncalcareous. Lithic arenites are a varied and inadequately defined class;

ISSN 2350-1049

International Journal of Recent Research in Interdisciplinary Sciences (IJRRIS)
Vol. 10, Issue 2, pp: (41-57), Month: April - June 2023, Available at: www.paperpublications.org

lots of rock bits of lithic sandstones are made up of materials that vary considerably in composition (Pettijohn, 1963). In addition to copious rock fragments of extensively diverse composition, numerous lithic arenites contain clay matrix with diverse compositions which can contain higher levels of Fe and Mg (Lindsey, 1999).

Based on the study of a reference set, Lindsey (1999) proposed the following guidelines for chemical classification of sandstones:

1) quartz arenite: Log (SiO_2/Al_2O_3) ≥ 1.5

2) graywacke: Log ($SiO_2/Al2O_3$) < 1 and Log (K_2O/Na_2O) < 0

3) arkose (includes subarkose): Log ($SiO_2/Al2O_3$) < 1.5 and Log (K_2O/Na_2O) ≥ 0 and Log ((Fe_2O_3+MgO)/(K_2O+Na_2O)) < 0

4) lithic arenite (subgraywacke, includes protoquartzite): Log ($SiO_2/Al2O_3$) < 1.5 and either Log (K_2O/Na_20) < 0 or Log ((Fe_2O_3+MgO)/(K_2O+Na_2O)) ≥ 0. If Log (K_2O/Na_2O) < 0, lithic arenite can be confused with graywacke.

Table 2: The chemical composition of Nanka sandstone (major oxides expressed in percentages (%), trace and REE in parts per million (ppm).

Oxides	AG1	AG2	NA1	NA2	NA3	OG1	OG2	OK1	OK2	OK3	Average	UCC
SiO_2	92.42	93.82	94.35	94.68	95.33	97.18	94.66	96.58	97.78	93.95	95.08	65.89
Al_2O_3	3.91	3.55	3.19	2.94	2.32	0.38	2.68	1.30	0.50	2.63	2.34	15.17
Fe_2O_3	1.00	0.36	0.47	0.50	0.30	0.94	0.55	0.46	0.55	0.58	0.57	5
MnO	0.00	0.01	0.01	0.01	0.01	0.00	0.01	0.01	0.00	0.01	0.01	0.07
MgO	0.04	0.03	0.04	0.04	0.03	0.03	0.04	0.07	0.04	0.12	0.05	2.2
CaO	0.02	0.02	0.02	0.02	0.02	0.02	0.01	0.04	0.02	0.03	0.02	4.19
Na_2O	0.00	0.00	0.00	0.00	0.00	0.00	0.00	0.01	0.00	0.07	0.01	3.9
K_2O	0.02	0.04	0.02	0.01	0.01	0.04	0.01	0.14	0.06	0.32	0.07	3.39
TiO_2	0.23	0.19	0.14	0.20	0.11	0.07	0.19	0.17	0.03	0.15	0.15	0.5
P_2O_5	0.02	0.01	0.01	0.01	0.01	0.01	0.02	0.02	0.01	0.02	0.01	0.2
LOI	1.86	1.48	1.25	1.23	0.86	0.37	1.19	0.56	0.36	1.36	1.05	-
TRACE & RARE EARTH ELEMENTS												
V	20.75	11.31	8.2	13.9	7.51	9.57	13.05	11.9	6.54	13.1	11.58	107
Cr	26.1	14.55	18.4	59.5	17.9	15.15	22.05	13.35	7.2	25.25	21.95	85
Co	233	282.3	278.75	257.1	317.85	352.4	235.75	346.15	289.35	417.5	301.02	17
Ni	16.25	17.35	22.5	39.95	20.4	20.25	20.75	22.5	19.5	33.9	23.34	20
Cu	19	24.35	11.28	31.65	4.93	16.85	12.1	21.1	15.55	5.53	16.23	25
Zn	7.25	11.7	11	11.3	13.2	12.15	7.5	8.7	11.05	18.45	11.23	71
Zr	122.05	235.2	151.35	166	90.5	46.85	139.5	155.8	50.6	127.75	128.56	190
Nb	7.07	8.86	4.23	5.31	3.2	1.03	3.82	4.55	1.32	4.9	4.43	12
Mo	1.31	0.47	0.52	0.65	0.44	0.25	0.31	0.4	0.27	0.5	0.51	1.5
Hf	2.9	5.6	3.26	3.7	2.62	1.35	3.32	3.56	1.44	3.12	3.09	5.8
Ta	0.43	0.68	0.29	0.42	0.23	0.09	0.25	0.32	0.12	0.33	0.32	1
Rb	0.95	1.85	0.82	0.84	0.8	1.09	0.59	3.26	1.57	8.39	2.02	112.2
Sr	8.3	6.69	8.34	7.33	7.56	10.01	16.82	11.45	7.03	18.59	10.21	350
Cs	0.25	0.26	0.00	0.00	0.00	0.00	0.00	0.00	0.00	0.3	0.08	4.6
Ba	23.8	35.65	35.1	27	39.65	46	46.3	121.5	122.45	203.55	70.10	550
Pb	4.78	7.82	8.21	9.57	8.65	4.04	8.42	3.68	3.96	7.02	6.62	17
Th	2.87	3.4	1.82	2.88	1.14	0.89	2.4	1.86	1.05	1.72	2.00	10.7
U	0.84	0.93	0.59	0.7	0.47	0.28	0.49	0.4	0.31	0.54	0.56	2.8
Sc	10.42	9.23	8.4	8.61	8.14	7.02	8.49	9.26	8.46	8.57	8.66	13.60
Y	3.62	6.72	2.61	4.28	2.18	1.41	2.64	8.7	1.49	5.59	3.92	22
La	7.43	6.35	6.17	9	6.31	2.89	10.22	4.35	2.4	7.91	6.30	30
Ce	21.61	12.84	18.42	36.25	12.87	5.37	17.77	15.07	5.19	60.05	20.54	64
Pr	1.24	1.52	0.97	1.5	1.27	0.55	1.77	1	0.5	1.63	1.20	7.1
Nd	3.51	5.31	3.29	5.65	4.68	2.08	6.72	4.46	1.89	6.24	4.38	26
Sm	0.67	1.09	0.46	1.04	0.79	0.35	0.94	0.83	0.43	1.37	0.80	4.5
Eu	0.11	0.21	0.06	0.19	0.22	0.06	0.18	0.2	0.08	0.3	0.16	0.88
Gd	0.38	1.1	0.59	1.02	0.52	0.22	0.68	0.98	0.31	1.47	0.73	3.8
Tb	0.11	0.19	0.1	0.17	0.09	0.05	0.12	0.2	0.05	0.21	0.13	0.64
Dy	0.59	1.11	0.5	0.74	0.53	0.25	0.56	1.39	0.39	1.11	0.72	3.5

ISSN 2350-1049

International Journal of Recent Research in Interdisciplinary Sciences (IJRRIS)
Vol. 10, Issue 2, pp: (41-57), Month: April - June 2023, Available at: www.paperpublications.org

Ho	0.11	0.26	0.11	0.18	0.11	0.05	0.12	0.33	0.09	0.21	0.16	0.8
Er	0.43	0.79	0.3	0.44	0.27	0.13	0.37	0.75	0.18	0.57	0.42	2.3
Tm	0.06	0.11	0.05	0.08	0.08	0.05	0.06	0.1	0.07	0.12	0.08	0.33
Yb	0.69	0.84	0.42	0.48	0.35	0.12	0.39	0.73	0.19	0.63	0.48	2.2
Lu	0.08	0.15	0.12	0.09	0.06	0.00	0.06	0.1	0.07	0.12	0.09	0.32

The Nanka Sandstone has Log (SiO_2/Al_2O_3) values ranging between 1.37 and 2.41 with an average of 1.71; Log (K_2O/Na_2O) between 1.15 and 0.66 (average = 0.90) and Log ((Fe_2O_3+MgO)/(K_2O+Na_2O)) ranging from 1.79 to 59 with an average of 27.27. based on the aforementioned values and using Lindsey (1999) criteria, the Nanka sandstone classified as quartz arenites.

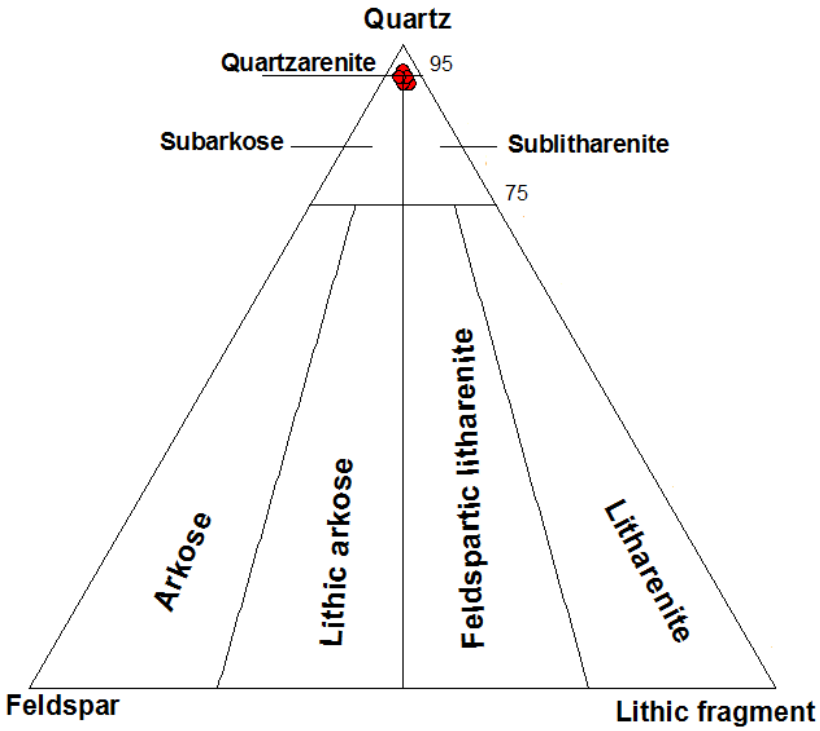

Figure 3: QFL ternary classification plot of the Nanka sandstone (after Folk, 1974).

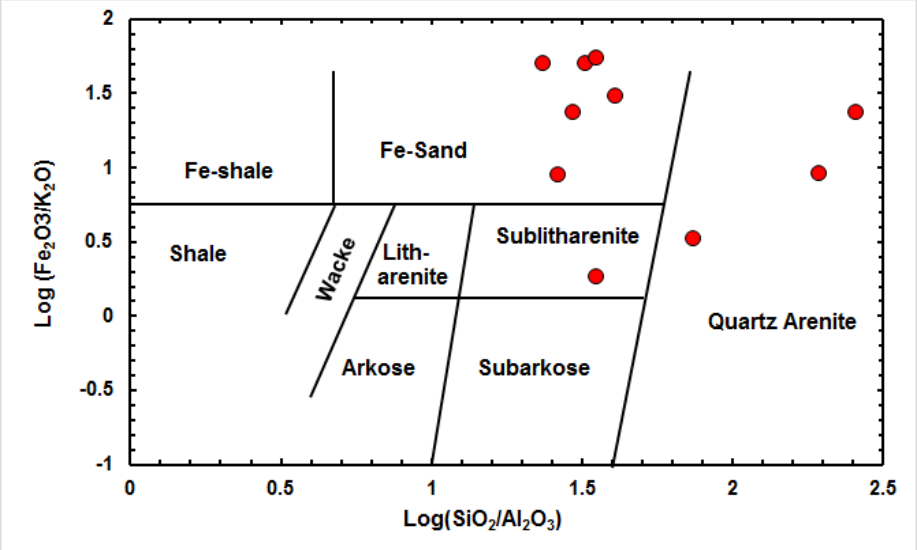

Figure 4. SandClass system for geochemical classification of the Nanka sandstone. The third axis, not shown, is the Ca content, dividing samples into noncalcareous (Ca < 4%), calcareous (4% < Ca < 15%), and carbonate (Ca > 15%) sediments (After, Herron (1988).

ISSN 2350-1049

International Journal of Recent Research in Interdisciplinary Sciences (IJRRIS)
Vol. 10, Issue 2, pp: (41-57), Month: April - June 2023, Available at: www.paperpublications.org

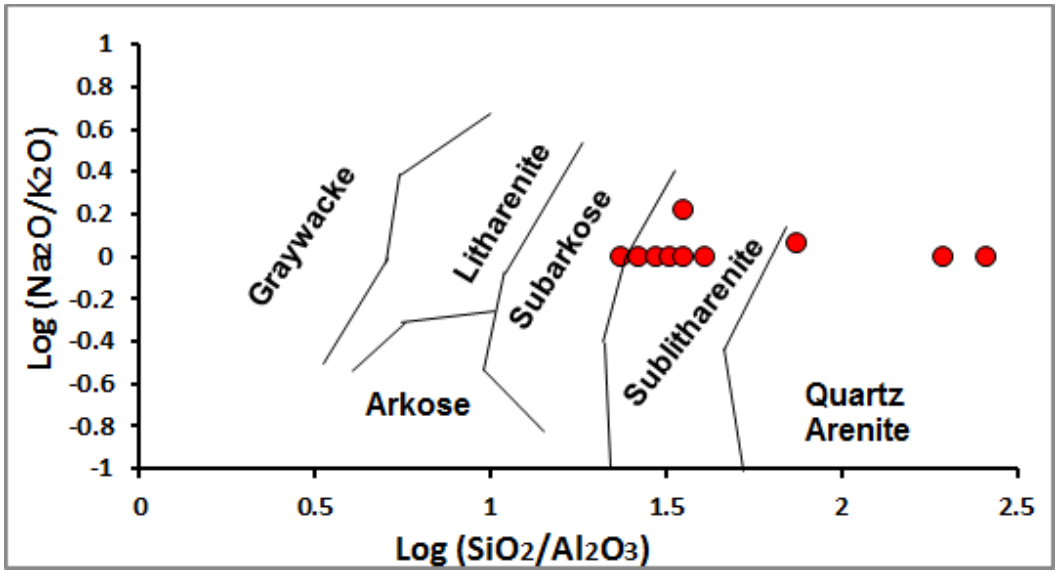

Figure 5. Chemical classification of the Nanka sandstone based on diagram of Pettijohn *et al.* (1972).

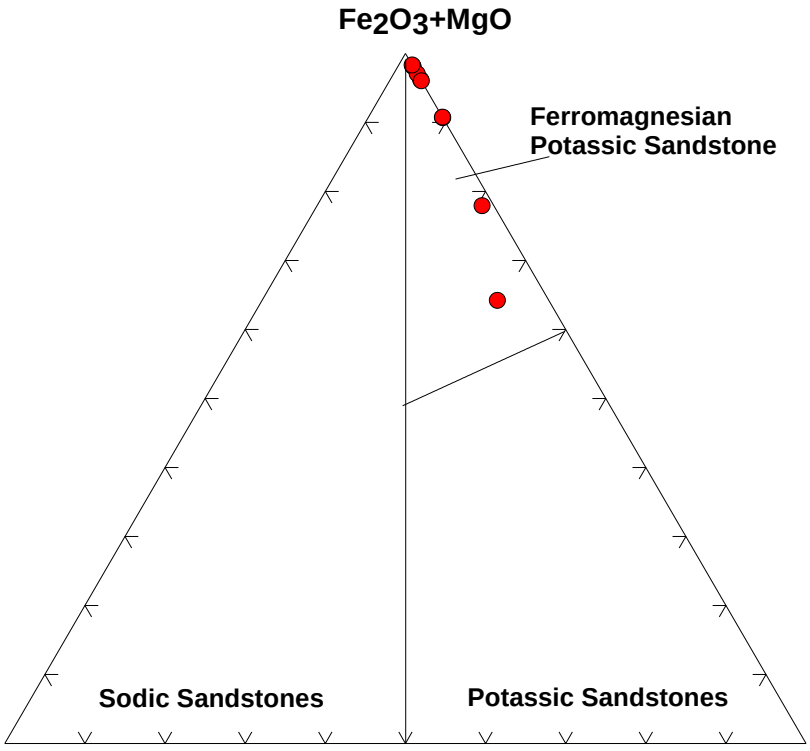

Figure 6: Ternary diagram of Na_2O-K_2O-(Fe_2O_3+MgO), after Blatt et al., (1972).

4.2 Maturity

The contents of quartz, rock fragments, feldspars and grain size can be used to interpret sandstone maturity. As the proportion of quartz increases so does the mineralogical maturity. Maturity can be exhibited in finer grain sizes; though, it is essentially clay content that is more directly related to lack of mineralogical maturity. Sandstones typically contain clay minerals developing on the surface of the grains or lining and occasionally filling the pore space (Prothero and Schwab, 2004). Maturity of sandstones can be revealed by the SiO_2/Al_2O_3 index. High ratios indicate mineralogically mature (quartzose, rounded) sandstones, while low ratios represent chemically immature samples (Potter, 1978). SiO_2/Al_2O_3 ratios of clastic rocks are sensitive to sediment recycling and weathering process and can be used as an indicator of sediment maturity. With increasing sediment maturity, quartz survives preferentially to feldspars, mafic minerals and lithics (Roser

and Korsch, 1986; Roser et al., 1996). The very high values of the ratio of SiO_2/Al_2O_3 for the Nanka sandstone (23.64 – 255.74) indicate that all the samples have low degree of clayness, which suggests mineralogical maturity. The alkali content (Na_2O+K_2O) is a measure of the feldspar constituent and can be used for index of chemical maturity. The Na_2O+K_2O content for the studied sandstone range from 0.01 to 0.4, indicating the near absence of feldspar and high chemical maturity. According to Farquhar et al (2014), samples with low SiO_2/Al_2O_3 ratio and a higher Fe_2O_3/K_2O ratio should be mineralogically less stable and more prone to reactivity during supercritical CO_2 exposure. The Nanka sandstone has high SiO_2/Al_2O_3 and Fe_2O_3/K_2O ratios and are mineralogically mature.

Detrital mineralogy can be determined by the Index of compositional variation (ICV) and ratio of K_2O/Al_2O_3 (Cox *et al.*, 1995); ICV is defined as: $(Fe_2O_3+Na_2O+CaO+MgO+TiO_2)/Al_2O_3$. More matured sandstone with mostly clay minerals displays lower ICV values that are less than 1.0 and such sandstones are derived from cratonic environment (Cox et al., 1995). The Nanka sandstone has and average ICV value of 0.65 indicating mineralogical maturity.

Gill and Yamane (1996) proposed that the stability of mobile oxides can be determined by $Al_2O_3/(CaO+MgO+Na_2O+K_2O)$ ratio. The Nanka sandstones revealed high positive values (4.17 to 48.88), indicating the presence of stable mobile oxides and mineralogical maturity. The Presence of calcite is the most common cement in sandstone, although when present it does not fill all pore spaces completely but occurs as patchy cement. $CaO+MgO/Al_2O_3$ molecular weight can be utilised to determine calcification (Gill and Yamane, 1996). The Nanka samples have $CaO+MgO/Al_2O_3$ values ranging between 0.01 and 0.13, which indicates that the sandstones are less calcified and thus chemically mature.

Figure 7 shows the ratio of SiO_2/Al_2O_3 plotted against that of quartz/(feldspar + lithic fragments). Pettijohn (1975) interpreted these ratios to reflect the maturity of sandstones. Higher SiO_2 ratio coincides with higher silica phases of quartz, quartzite and chert which in turn reflects that such sandstones are mature (Al-Juboury, (2007). From Figure 7, the Nanka sandstone exhibited high SiO_2 and are mature.

The ZTR index is expressed in percentage and is a measure of the maturity of a heavy mineral suite (Pettijohn et al., 1972). Table 3 shows the heavy mineral data and the ZTR Index of the Nanka sandstone. The ZTR ratio appraises the degree of dissolution that has occurred in the sediment (Hubert, 1962). The ZTR index was computed using the percentage of the collective zircon, tourmaline and rutile grains for each sample based on Hubert's (1962) formula:

$$\textbf{ZTR Index} = \frac{Zircon+Tourmaline+Rutile}{Total\ number\ of\ Non\ opaque\ heavy\ minerals}$$

In greywackes and arkoses, the ZTR index is between 2-39%, and usually exceeds 90% in quartz arenites (Mange and Maurer, 1992). ZTR <75% implies immature to sub mature sediments and ZTR >75% indicates mineralogically matured sediments; typically, ZTR index values of between 75 and 88% are characteristics of mature sediments. The ZTR Index for the Nanka sandstone range between 59.38 to 65.52% with an average of 62.59%, the ZTR indices imply that the Nanka sandstone is mineralogically immature to sub mature. Table 4 shows the modal composition and the mineralogical maturity index (MMI) of the samples studied and the classification is based on the parameters in Table 5. The mineralogical maturity index is determined using the expression:

$$MMI = \frac{\text{Proportion of Qtz}}{\text{Proportion of Fsp} + \text{Proportion of R. F}}$$

The MMI values for the Nanka sandstone range from 15 and 23 with an average of 18 suggesting the sediments to be mature to super mature.

4.3 Geochemistry

SiO_2 is the dominant oxide in the Nanka sandstone, it ranges between 92.42 and 97.66% (Av. 95.08%), Silica enrichment is a measure of sandstone maturity; an indication of the period and extent of weathering and removal of other minerals during transportation (Lindsey, 1999). According to Lindsey (1999), silica enrichment also occurs by addition of silica cement, as quartz and opal. Fe_2O_3 values ranges between 0.3 and 1% indicating intense chemical weathering; according to Lindsey (1999), the concentration of iron oxide (Fe_TO_3, total iron as Fe_2O_3) is the ultimate effect of provenance and processes that concentrate and preserve detrital ferromagnesian and iron minerals (mainly amphibole,

ISSN 2350-1049

International Journal of Recent Research in Interdisciplinary Sciences (IJRRIS)
Vol. 10, Issue 2, pp: (41-57), Month: April - June 2023, Available at: www.paperpublications.org

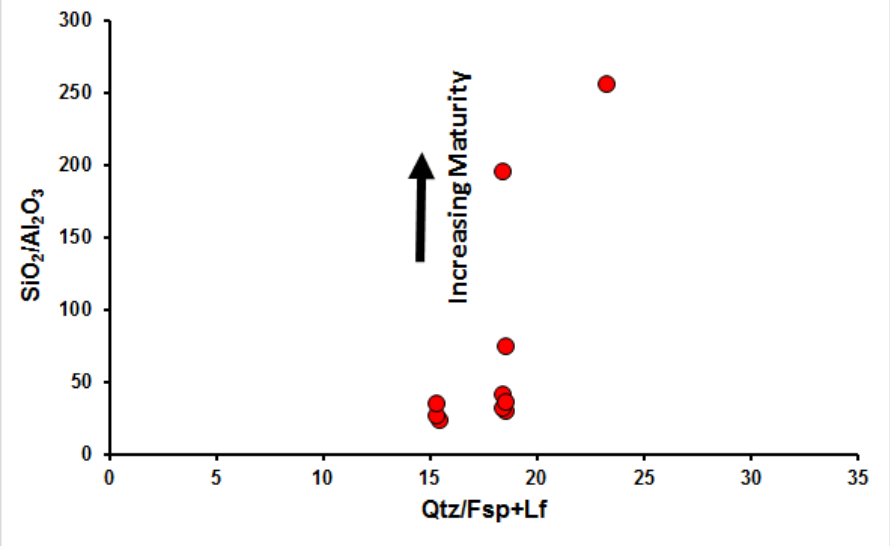

Figure 7. The ratio SiO_2/Al_2O_3 and Qtz/ (Fsp+Lf) (total quartz)/(feldspar + lithic fragments) in the Nanka sandstone, adapted from Al-Juboury, (2007).

Table 3. Heavy mineral data and the ZTR Index of the Nanka sandstone

Sample ID	Zircon	Rutile	Tourmaline	Sillimanite	Garnet	Apatite	Opaque	Total ZTR	Total Non opaque	ZTR Index (%)
AG1	6	6	7	5	3	3	22	19	30	63.33
AG2	6	5	7	4	2	4	23	18	28	64.29
NA1	7	4	5	4	4	2	25	16	26	61.54
NA2	7	4	5	4	3	3	24	16	26	61.54
NA3	6	7	6	5	3	2	22	19	29	65.52
OG1	5	6	7	2	5	3	23	18	28	64.29
OG2	6	6	5	3	3	4	23	17	27	62.96
OK1	7	6	8	4	5	4	21	21	34	61.76
OK2	8	6	5	5	4	4	24	19	32	59.38
OK3	6	7	6	3	4	5	22	19	31	61.29
Average	**6.40**	**5.70**	**6.10**	**3.90**	**3.60**	**3.40**	**22.90**	**18.20**	**29.10**	**62.59**

Table 4. Modal composition of the Nanka sandstone and the Mineralogical Maturity Index.

Sample ID	Quartz (Qtz)	Feldspar (Fsp)	Rock (Lithic) Fragment (RF)	Fsp+RF	Mineralogical Maturity Index (MMI)
AG1	93	2	4	6	16
AG 2	92	3	3	6	15
NA1	93	3	2	5	19
NA2	92	2	3	5	18
NA3	92	3	2	5	18
OG1	93	2	2	4	23
OG2	92	3	3	6	15
OK1	93	3	2	5	19
OK2	92	2	3	5	18
OK3	93	3	2	5	19
Average	**92.5**	**2.6**	**2.6**	**5.20**	**18**

ISSN 2350-1049

International Journal of Recent Research in Interdisciplinary Sciences (IJRRIS)
Vol. 10, Issue 2, pp: (41-57), Month: April - June 2023, Available at: www.paperpublications.org

Table 5. Maturity scale of sandstone: Limiting % of Q and (F + RF) MI and maturity stage (Nwajide and Hoque, 1985).

Q ≥ 95% (F + RF) = 5%	MI ≥ 19 (Supermature)
Q = 95 - 90% (F + RF) = 5 - 10%	MI = 19 - 9 (Mature)
Q = 90 - 75% (F + RF) = 10 - 25%	MI = 9 - 3 (Submature)
Q = 75 - 50% (F + RF) = 25 - 50%	MI = 3 - 1 (Immature)
Q < 50%	MI ≤ 1
(F + RF) > 50%	Extremely immature

mica, illite, ilmenite, and magnetite) and their alteration products (chlorite, hematite, and some clays). Concentration of detrital ferromagnesian minerals reflects their abundance in source rocks and is increased by hydraulic sorting and is decreased by chemical destruction during weathering and diagenesis under oxidizing conditions (Lindsey, 1999). Al_2O_3 values are from 0.38 to 3.91% and is due to weathering effects. Na_2O and K_2O have values ranging from 0 to 0.07 and 0.01 and 0.32 respectively, indicating the removal of alkali elements. CaO ranges from 0.01-0.04%; indicating a lack of calcite cement.

Harker diagrams are valuable in comparing the abundances of the major oxides along a common axis. A decrease in the abundance of TiO_2, Fe_2O_3, CaO, Na_2O, MgO, MnO, K_2O, and Al_2O_3 as SiO_2 increases was the trend observed (Fig. 8), this could be due to chemical weathering and removal of these elements. As shown in Figure 9A, there is no correlation between K_2O and TiO_2 suggesting a loss of K_2O which is an indication of diagenetic alteration of feldspars. The plot of SiO_2 vs Na_2O (Fig. 9B) shows that there is also no correlation with Na; the extrapolated regression equation did not pass through the origin, suggesting minimal Na_2O contribution from the clay minerals. K_2O is contained mainly by the clay minerals, a loss of K_2O associated with feldspar alteration produces a detectable scatter plot (Spears and Amin, 1981).

There is no correlation between TiO_2 and Al_2O_3 (Fig. 10A), attributable to the depositional process and granulometry; indicating that TiO_2 is not associated with phyllosilicates. TiO_2/Al_2O_3 ratio is between 0.11 and 1.92 (av. 0.41); as the grain size of the sediment decreases this ratio decreases (Spears & Kanaris-Sotiriou, 1975). This low value suggests that the sandstone matrix is composed of clay minerals.

There is an almost nil negative correlation between K_2O and Al_2O_3 (Fig. 10B) as a result of changes in the quartz-matrix proportions, which according to Spears and Amin (1981) is due to grain-size-related quartz variations reflecting the grading. From figure 11, only Co from the samples studied showed very high enrichment compared to UCC, PAAS and NASC, which may indicate the felsic nature of the source rock. Ba and Sr have values much lower than that of the UCC, PAAS and NASC.

According to Schrijver et al (1994), depletion of Ba may be due to leaching of barium from feldspar penecontemporaneous with feldspar dissolution. Because of its high mobility, Sr is readily removed from parent rocks during chemical weathering (Yang et al., 2004). The distribution of Sr during sedimentary processes is affected by strong adsorption on clay minerals and is easily mobilised during weathering, especially in oxidizing acid environments, and naturally incorporated in clay minerals (Kovács, 2007). Figure 12 is a spidergraph of rare earth elements concentration of the Nanka sandstone relative to of the UCC, PAAS and NASC; the Nanka sandstone is depleted in REE due to the dilution effect of quartz. The UCC, PAAS and NASC-normalized plot for the trace elements in the Nanka sandstone is shown in Figure 13; the UCC, PAAS and NASC has similar pattern and shows the marked enrichment of Co. Figure 14 is the UCC, PAAS and NASC-normalized plot for the rare earth elements in the Nanka sandstone showing an almost flat pattern for all the compositional standards indicating depletion of these elements.

The Al—Ti—Zr ternary diagram can be applied in accessing the effects of sorting processes, zircon concentration and sediment maturity (Garcia et al. 1994). According to Asiedu et al (2000), mature sediments consisting of both sandstones and shales show a wide range of TiO_2/Zr variations, whereas immature sediments of sandstones and shales show a more limited range of TiO_2/Zr variations. Figure 15 shows the Nanka sandstone plotting only in the sandstone zone close to the zircon apex with a wide range of TiO_2/Zr variations, indicating compositional maturity, good sorting trend, rapid deposition and low to medium Zr concentration. The ternary plot (Fig. 16) can be used to determine whether there has been any significant accumulation of either zircon or titanite which would be denoted by a trend towards the Hf apex. The Nanka sandstone plotted not too far from the Hf area, which implies low to moderate accumulation of heavy minerals. However,

ISSN 2350-1049

International Journal of Recent Research in Interdisciplinary Sciences (IJRRIS)
Vol. 10, Issue 2, pp: (41-57), Month: April - June 2023, Available at: www.paperpublications.org

the ternary diagram (Fig. 17) shows the Nanka sandstone plotting close to the average oceanic crust plot far from the Hf apex which suggests minute or no accumulation of heavy minerals (e.g. zircon) rich in Hf.

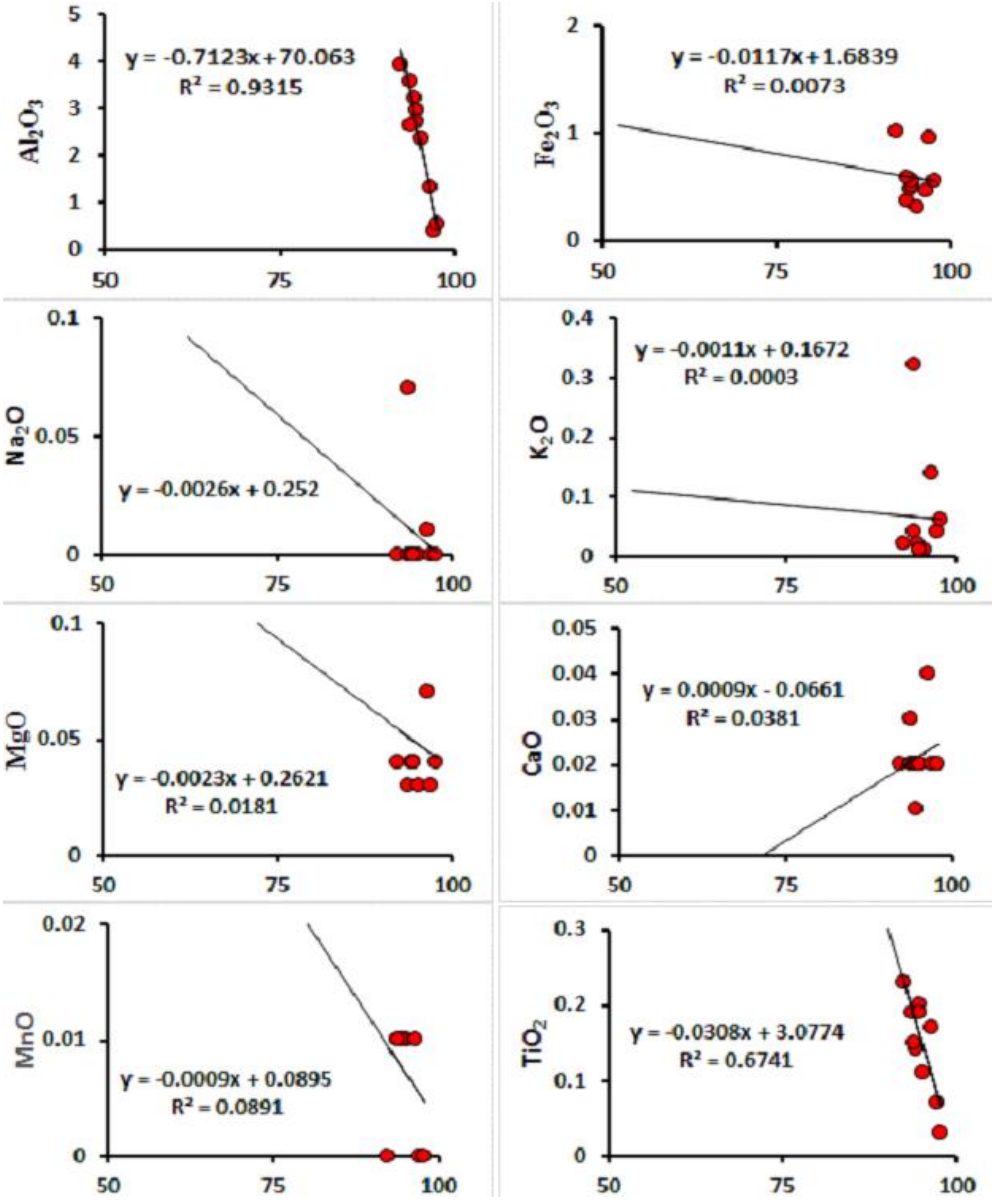

Figure 8. Harker diagram of major elements plotted against SiO_2 of the studied samples.

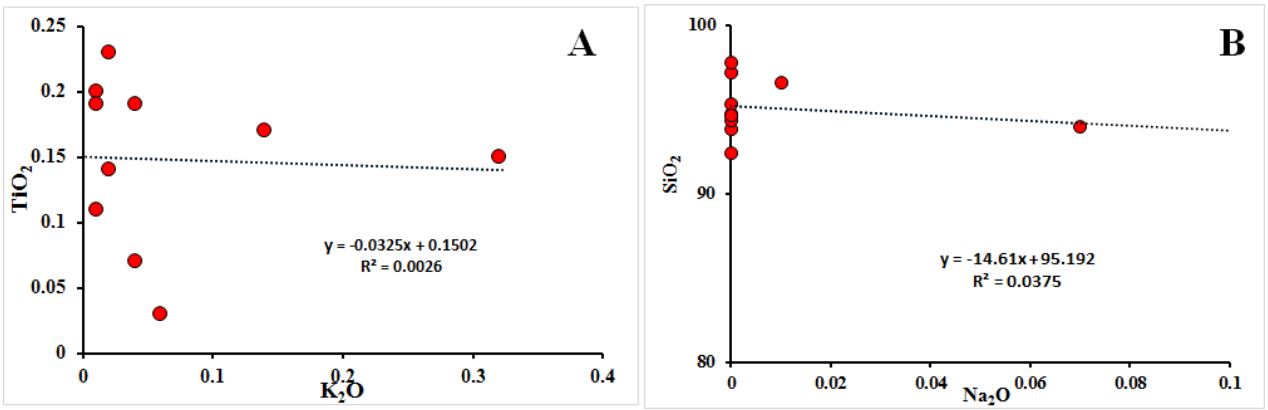

Figure 9. (A) Plot of K_2O against TiO^2 and (B) Na_2O against SiO_2 for the Nanka sandstone

ISSN 2350-1049

International Journal of Recent Research in Interdisciplinary Sciences (IJRRIS)
Vol. 10, Issue 2, pp: (41-57), Month: April - June 2023, Available at: www.paperpublications.org

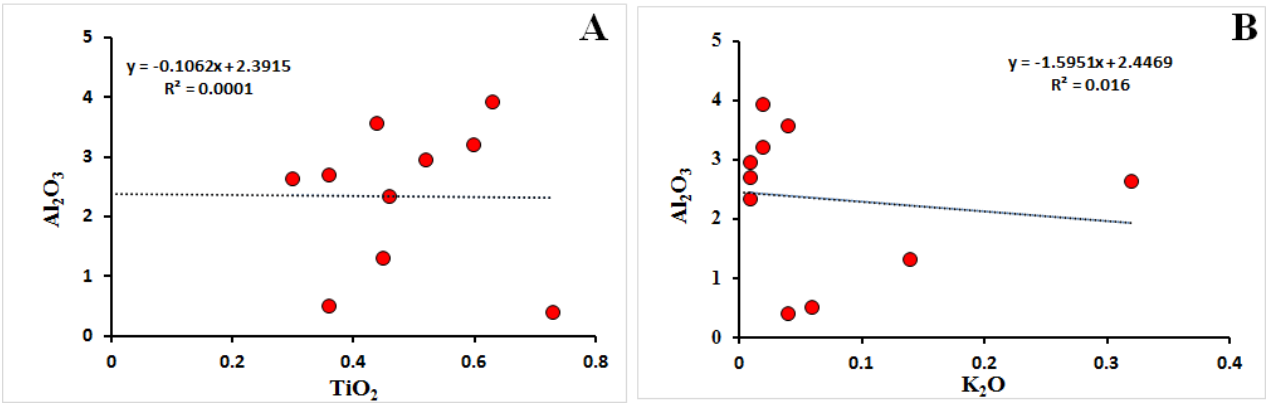

Figure 10. Correlation plots of (A) TiO_2 vs AI_2O_3 and (B) K_2O against AI_2O_3

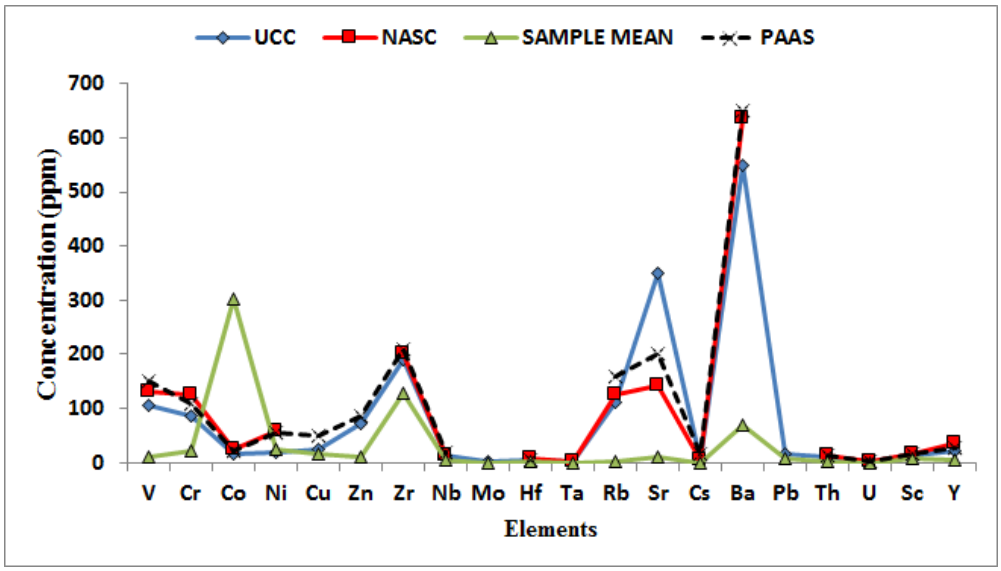

Figure 11. Spidergraph of the mean concentration of trace elements in the Nanka sandstones relative to the UCC, PAAS and NASC. PAAS = Post-Archaean Australian Shale; UCC = Upper Continental Crust (data from Taylor and McLennan, 1985) and NASC = North American Shale Composite (data from Gromet et al., 1984).

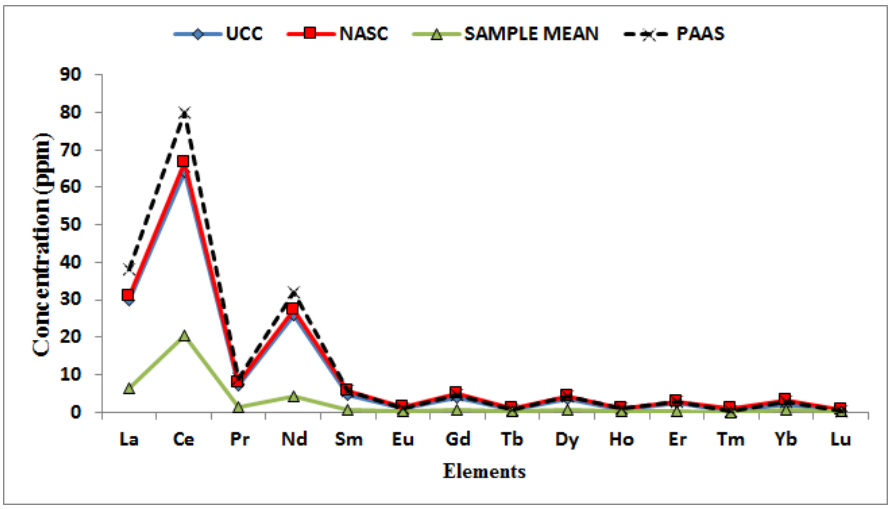

Figure 12. Spidergraph of the mean concentration of rare earth elements in the Nanka sandstones relative to the UCC, PAAS and NASC. PAAS = Post-Archaean Australian Shale; UCC = Upper Continental Crust (data from Taylor and McLennan, 1985) and NASC = North American Shale Composite (data from Gromet et al., 1984).

ISSN 2350-1049

International Journal of Recent Research in Interdisciplinary Sciences (IJRRIS)
Vol. 10, Issue 2, pp: (41-57), Month: April - June 2023, Available at: www.paperpublications.org

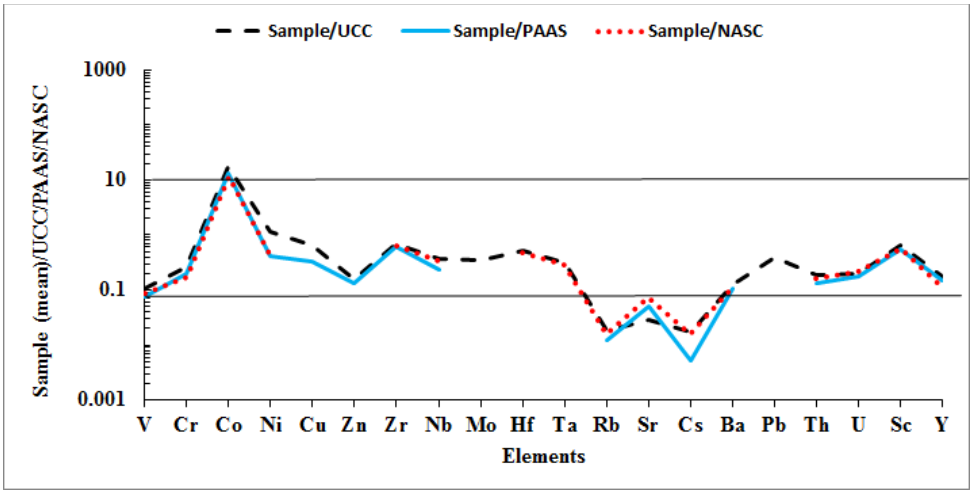

Figure 13. UCC-PAAS-NASC normalized spidergraph for trace elements from the Nanka sandstone.

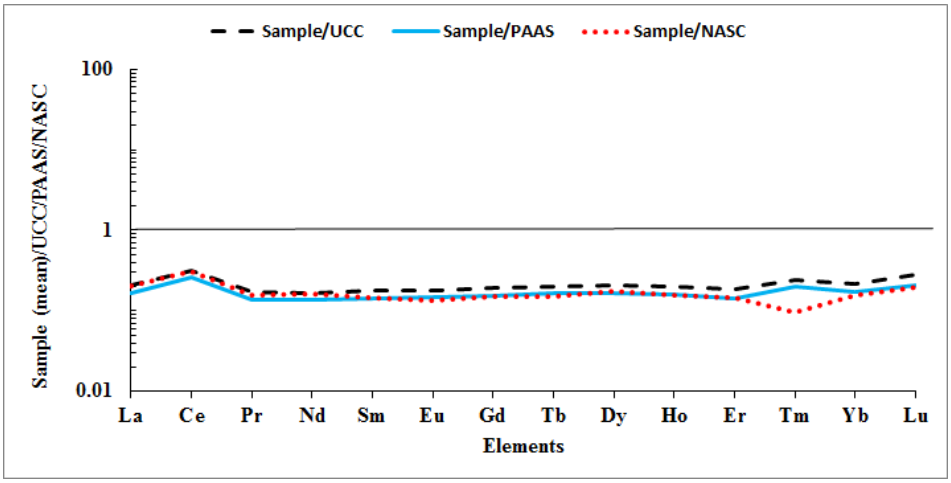

Figure 14. UCC-PAAS-NASC normalized spidergraph for REEs from the Nanka sandstone

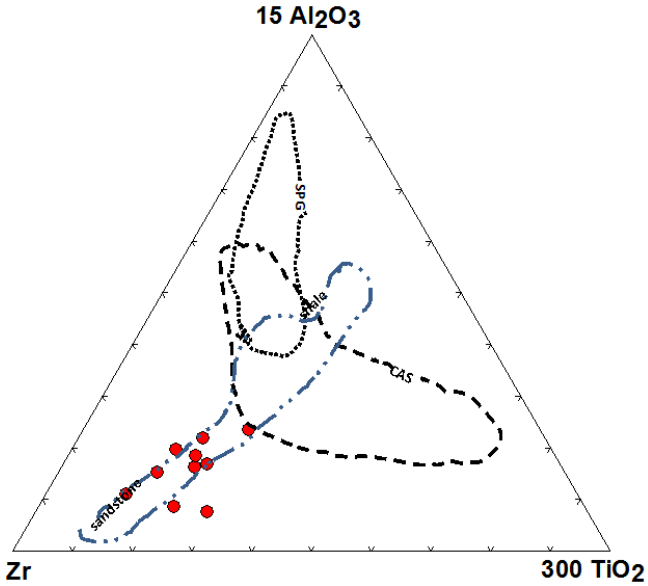

Figure 15. Al—Ti—Zr plot for the Nanka sandstone. The sandstone-shale contour refers to the observed range of compositions in clastic sediments. CAS refers to the fields of calc-alkaline suites and SPG refers to fields of strongly peraluminous granites (after Garcia et al. 1994)

ISSN 2350-1049

International Journal of Recent Research in Interdisciplinary Sciences (IJRRIS)
Vol. 10, Issue 2, pp: (41-57), Month: April - June 2023, Available at: www.paperpublications.org

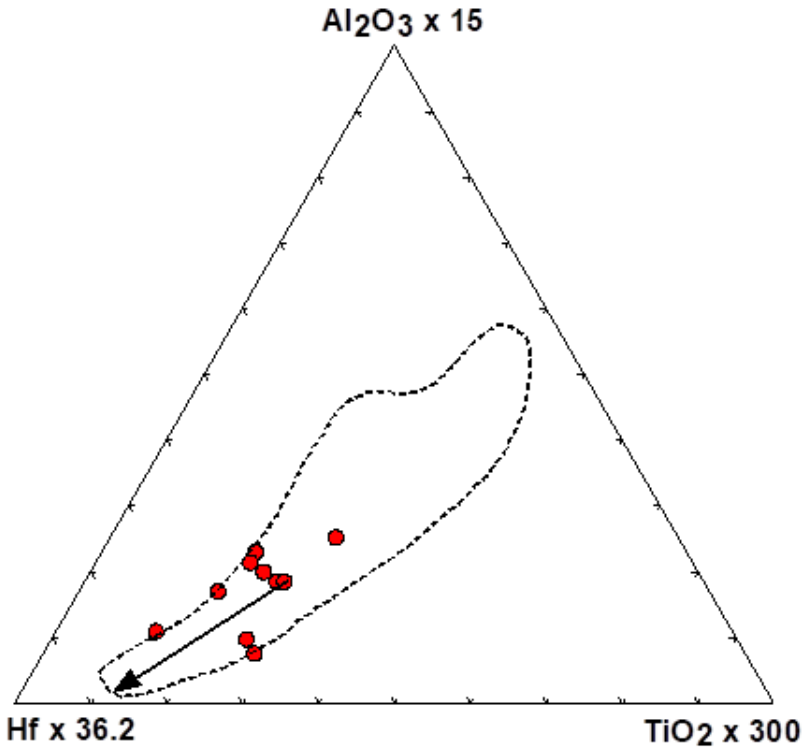

Figure 16: Al_2O_3 *15 - Hf*36.2 – TiO_2*300 plot. Field after La Fléche and Camiré (1996) and Garcia et al. (1994). The arrow indicates sorting trend.

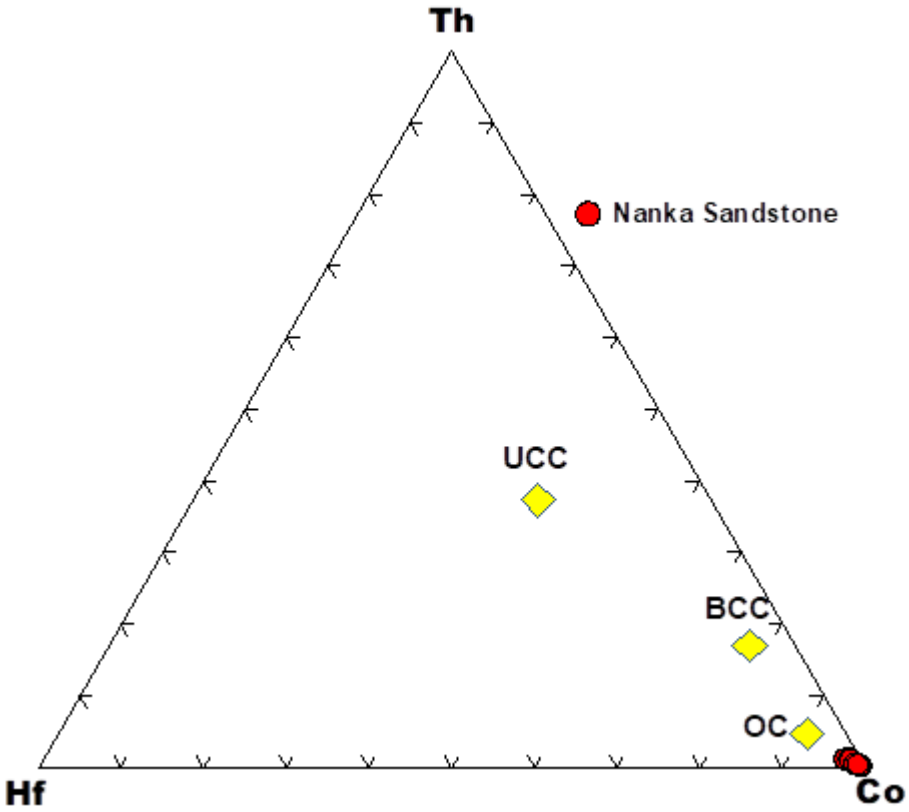

Figure 17: Th-Hf-Co plot. Fields after Taylor and McLennan (1985). UCC = Upper continental crust; BCC = bulk continental crust; OC = average oceanic crust

5. CONCLUSIONS

The Nanka sandstones are non-calcareous, ferromagnesian potassic sandstones composed of sublitharenites and quartz arenites. The SiO_2/Al_2O_3 and Fe_2O_3/K_2O ratios are high, suggesting mineralogical maturity and low degree of clayness with stable mobile oxides present. The alkali (Na_2O+ K_2O) content of the studied sandstone indicates the near absence of feldspar and high chemical maturity. The Nanka sandstone has an average ICV value of 0.65 indicating mineralogical maturity. The plot of ratio SiO_2/Al_2O_3 against quartz / (feldspar + lithic fragments) shows that the sandstones are mature. The ZTR values suggests that the sediments are mineralogically immature to sub mature. The mineralogical maturity index (MMI) classifies the Nanka sandstone as mature to super mature. A decrease in the abundance of TiO_2, Fe_2O_3, CaO, Na_2O, MgO, MnO, K_2O, and Al_2O_3 as SiO_2 increases was the trend observed, and could be attributed to chemical weathering and removal of these elements. There is no correlation between K_2O and TiO_2 suggesting a loss of K_2O which is an indication of diagenetic alteration of feldspars. There is also no correlation with Na; the extrapolated regression equation did not pass through the origin, suggesting minimal Na_2O contribution from the clay minerals.

There is no correlation between TiO_2 and Al_2O_3 due to depositional process and granulometry; indicating that TiO_2 is not associated with phyllosilicates. The TiO_2/Al_2O_3 ratio is low indicating that the sandstone matrix is composed of clay minerals. There is no correlation between K_2O and Al_2O_3 due to changes in the quartz-matrix proportions reflecting the grading. The Al—Ti—Zr ternary diagram shows the Nanka sandstone plotting close to the zircon apex with a wide range of TiO_2/Zr variations, indicating compositional maturity, good sorting trend, rapid deposition and low to medium Zr concentration. Al_2O_3 *15-Hf*36.2 – TiO_2*300 and Th-Hf-Co ternary plots indicate which implies low to moderate accumulation of heavy minerals.

ACKNOWLEGDEMENT

The author sincerely acknowledges Dr. A. B. Eluwole for his contribution in the production of location map of the study area and students who participated in the field work.

REFERENCES

[1] Adegoke, O.S., 1969. Eocene Stratigraphy of Southern Nigeria: Colloque sur l' Eocene, III. Bureau de Recherché Geologiques et Minieres, 69, 20 – 48.

[2] Agagu, O. K. & Adighije, C. I., 1983. Tectonic and sedimentation framework of the lower Benue Trough, Southern Nigeria. Journal of African Earth Science. 1/3-4, 267-274.

[3] Agagu, O.K., Fayose, E.A., Petters, S.W., 1985. Stratigraphy and sedimentation in the Senonian Anambra Basin of eastern Nigeria. Journal of Mining and Geology, 22/1, 25-36.

[4] Al-Juboury A.I. (2007). Petrography and major element geochemistry of Late Triassic Carpathian Keuper sandstones: Implications for provenance. Bulletin de l'Institut Scientifique, Rabat, section Sciences de la Terre, n°29, 1-14.

[5] Asiedu D.K., Suzuki S., Nogami K. & Shibata T., 2000. Geochemistry of Lower Cretaceous sediments, Inner Zone of Southwest Japan: Constraints on provenance and tectonic environment. *Geochemical J.* 34/2, 155—173..

[6] Benkhelil, M.J., 1982. Benue Trough and Benue chain. Geological Magazine, 119/2, 155-168.

[7] Benkhelil, M.J., 1987. Cretaceous deformation, magmatism and metamorphism in the lower Benue Trough, Nigeria. Geological Journal, 22/S2, 467-493.

[8] Blatt, H., Middleton, G., & Murray, R., 1972. Origin of sedimentary rocks. Prentice-Hall, Englewood Cliffs, New Jersey, 634 pp.

[9] Burke, K.C., Dessauvagie, T.F.J., Whiteman, A.J., 1972. Geological history of the Benue valley and adjacent areas. In: Dessauvagie, T.F.J., Whiteman, A.J. (Eds.), African Geology. University of Ibadan, Nigeria, pp. 187-206.

[10] Dessauvagie, T.F.J., 1975. Explanatory note, the geological map of Nigeria. Nigerian Journal of Mining and Geology, 9, 1-28.

[11] Cox, R., Lowe, D.R. & Cullers, R.L., 1995. The influence of sediment recycling and basement composition on evolution of mudrock chemistry in the southwestern United States. Geochimica et Cosmochimica Acta 59/14, 2919–2940.

[12] Ekine, A.S. and Onuoha, K.M., 2008. Burial history analysis and subsidence in the Anambra Basin, Nigeria. Nigerian Journal of Physics, 20/1, 145-154.

[13] Farquhar, S.M., Pearce, J.K., Dawson, G.K.W., Golab, A., Sommacal, S., Kirste, D., Biddle, D., Golding, S.D., 2014. A fresh approach to investigating CO2 storage: Experimental CO2-water-rock interactions in a low-salinity reservoir system, Chemical Geology, 399, 98-122.

[14] Flèche, M.R. and Camiré, G., 1996. Geochemistry and provenance of metasedimentary rock from the Archean Golden Pond sequence (Casa Berardi mining district, Abitibi subprovince): Canadian Journal of Earth Sciences, 33/5, 676–690.

[15] Folk, R.L., 1974. Petrology of Sedimentary Rocks, Second Edition, Hemphill Press, Austin, TX, 182 pp.

[16] Garcia D., Fonteilles M. & Moutte J., 1994. Sedimentary fractionations between Al, Ti, and Zr and the genesis of strongly peraluminous granites. *J. Geol.* 102/4, 411-422.

[17] Gill, S. and Yemane, K., 1996. Implications of a lower Pennsylvanian Ultisol for equatorial Pangean climates and early, oligotrophic, forest ecosystems. *Geology*, 24/10, 905-908.

[18] Gromet, L.P., Dymek, R.F., Haskin, L.A. and Korotev, R. L., 1984. The 'North American Shale Composite': its compilation, major and trace element characteristics. Geochimica et Cosmochimica Acta, 48/12, 2469–2482.

[19] Herron, M.M., 1988. Geochemical classification of terrigenous sands and shales from core or log data: Journal of Sedimentary Petrology, 58/5, 820–829.

[20] Hubert, J.F., 1962. A zircon-tourmaline-rutile maturity index and the interdependence of the composition of heavy mineral assemblages with the gross composition and texture of sandstones. Journal of sedimentary petrology, 32/3, 440-450.

[21] Kovács, J., 2007. Chemical Weathering Intensity of the Late Cenozoic "Red Clay" Deposits in the Carpathian Basin. Geochemistry International, 45/10, 1056–1063.

[22] Ladipo, K.O., 1986. Tidal shelf depositional model for the Ajali Sandstone, Anambra Basin, Southern Nigeria. Journal of African Earth Sciences, 5/2, 177-185.

[23] Lindsey, D.A., 1999. An Evaluation of Alternative Chemical Classifications of Sandstones. *United* State Geological Survey Open-File Report 99-346, 26 pp.

[24] Mange, M.A. & Maurer, F.W., 1992. Heavy Minerals in Colour. Springer Netherlands, 147 pp.

[25] Murat, R.C., 1972. Stratigraphic and paleogeography of the cretaceous and lower tertiary sediments in southern Nigeria. In: Dessauvagie, T.F.J., Whiteman, A.J. (Eds.), Africa Geology. University of Ibadan Press, 251-266.

[26] Nichols, G., 2009. Sedimentology and stratigraphy (2nd ed.). Wiley-Blackwell. Publishing, London, 419 pp.

[27] Nwajide, C.S., 1979. A lithostratigraphic analysis of the Nanka sand, Southeastern Nigeria. Nigerian Journal of Mining and Geology, 16, 103-109.

[28] Nwajide, C.S., 1980. Eocene tidal sedimentation in the Anambra Basin, Southern Nigeria. Sedimentary Geology, 25/3, 189-207.

[29] Nwajide, C.S., & Hoque, M., 1985. Problem of classification and maturity. Evaluation of a diagnostically altered fluvial Sandstone. *Geologic on Nujibouw*, 64, 67-70.

[30] Nwajide, C.S., and Reijers, T.J.A., 1996. Sequences architecture in outcrops, examples from the Anambra Basin, Nigeria. Nigerian Association of Petroleum Explorationists Bulletin, 11/1, 23-32.

[31] Obaje, N. G., 2009. Geology and Mineral Resources of Nigeria (Lecture Notes in Earth Sciences 120). Springer-Verlag Berlin Heidelberg, 221pp.

[32] Obi, G.C., 2000. Depositional Model for the Campanian Maastrichtian Anambra Basin, Southern Nigeria [Ph.D. Thesis]. University of Nigeria, Nsukka, Nigeria, 299 pp.

[33] Ofoegbu, C., 1982. Evolution of Anambra Basin. Nigerian Journal of Mining and Geology. 5/6, 45-60.

[34] Ola-Buraimo, A.O., Akaegbobi, I.M., 2013b. Palynological evidence of the oldest (Albian) sediment in Anambra Basin, southeastern Nigeria. Journal of Biological and Chemical Research, 30/2, 387-408.

[35] Pettijohn, F. J., 1963, Chemical composition of sandstones—excluding carbonate and volcanic sands, *in* Fleischer, M., ed., Data of Geochemistry, sixth edition, U. S. Geological Survey Professional Paper 440-S: 21 pp.

[36] Pettijohn, F. J., 1975. Sedimentary Rocks, third edition: Harper & Row, New York, 628 pp.

[37] Pettijohn, F.J., Potter, P.E., & Siever, R., 1972. Sand and Sandstones. Springer-Verlag, New York, 618 pp.

[38] Potter, P.E., 1978. Petrology and chemistry of modern big river sands. The Journal of Geology, 86(4): 423–449.

[39] Prothero, D.R. and Schwab, F. L., 2004. Sedimentary Geology: an introduction to sedimentary rocks and stratigraphy (2nd ed.). W.H. Freeman and company, New York, 557 pp.

[40] Reyment, R.A. 1965. Aspects of the Geology of Nigeria: the stratigraphy of the Cretaceous and Cenozoic deposits. Ibadan University Press, badan, Nigeria, 144 pp.

[41] Roser, B. P., & Korsch, R. J., 1986. Determination of tectonic setting of sandstone-mudstone suites using SiO_2 content and K_2O/Na_2O ratio. The Journal of Geology 94/5, 635-650.

[42] Roser, B.P., Cooper, R.A., Nathan, S. and Tulloch, A.J., 1996. Reconnaissance sandstone geochemistry, provenance, and tectonic setting of the lower Paleozoic terranes of the West Coast and Nelson, New Zealand, New Zealand Journal of Geology and Geophysics, 39/1, 1-16.

[43] Schrijver, K., Zartman, R.E., & Williams-Jones, A.E., 1994. Lead and barium sources in Cambrian siliciclastics and sediment provenance of a sector of the Taconic Orogen, Quebec: a mixing scenario based on Pb-isotopic evidence. Applied Geochemistry, 9/4, .455-476.

[44] Odunze, S.O. and Obi, G.C., 2013. Sedimentology and sequence stratigraphy of the Nkporo Group (Campanian-Maastrichtian), Anambra Basin, Nigeria. Journal of Palaeogeography, 2/2, 192-208.

[45] Simpson, A., 1954. The Nigerian Coalfield: The Geology of Parts of Onitsha, Owerri and Benue Provinces Bulletin of Geological Survey of Nigeria, 24, 85 pp.

[46] Spears D.A. & Kanaris-Sotiriou, R., 1975. Titanium in some Carboniferous sediments from Great Britain. Geochimica et Cosmochimica Acta, 40/3, 345-351.

[47] Spears, D. A., & Amin, M. A., 1981. A Mineralogical and Geochemical Study of Turbidite Sandstones and Interbedded Shales, Mam Tor, Derbyshire, UK. Clay Minerals, 16, 333-345.

[48] Taylor, S. R. and McLennan, S. H., 1985. The Continental Crust: Its Composition and Evolution.

[49] Blackwell Scientific Publications, Oxford, 312 pp.

[50] Yang, S. Y., Jung, H. S. and Li, C. X., 2004. Two Unique Weathering Regimes in the Changjiang and Huanghe Drainage Basins: Geochemical Evidence from River Sediments. Sediment. Geol. 164/1 & 2. 19–34.